

Generalized Spherical Harmonic Approximation to Polarized Radiative Transfer. Computational aspects

Igor N. Polonsky^{a,b} Michael A. Box^b Meike Vogt^{c,b}

^a*Los Alamos National Laboratory, Space and Remote Sensing Sciences Group
(ISR-2), Los Alamos, NM 87545, USA*

^b*School of Physics, University of New South Wales, Sydney, NSW, 2052,
Australia*

^c*Section of Physics, Ludwig-Maximilians-Universität, München, Germany*

Abstract

In the present paper we have implemented the generalized spherical harmonics approximation (GSHA) to simulate polarized radiative transfer through the real geophysical and artificial media like clouds, aerosols, sea and ocean water.

The most important advantage of the GSHA is that after initial calculation it is possible to obtain any energetic and polarized characteristics of the radiance at any point within the medium. Additional advantage is that the GSHA allows one to make simulation for several sources during a single run.

The primary goal of the present paper is to develop a computationally efficient algorithm to calculate the radiance characteristics. To achieve this goal some additional approximation will be introduced, which does not affect the accuracy of the numerical simulation. The accuracy of this technique is verified and analyzed through comparison with known test data.

Key words: Radiative transfer equation; Polarization; Generalized spherical harmonic approximation

1 Introduction

Recent research has demonstrated that if a measurement of the energetic characteristics of the radiance is complemented by the corresponding mea-

Email address: polonsky@lanl.gov (Igor N. Polonsky).

surement of the polarization state this results in a possibility to retrieve physical characteristics of the scattering medium [1] and of coupled atmosphere-underlying surface system [2] with a higher degree of trustworthiness. In particular, the use of polarization allows one to distinguish between spherical and non-spherical particles. Moreover, the use of polarized light in imaging leads to increasing of reliability of inhomogeneities detection in the scattering medium [3] which is very important, for example, in medical imaging.

The effective use of polarized light requires that a model of radiance propagation through scattering media which takes into account the polarization effects be developed. Although the equation which governs this process has been known for more than 50 years [4,5] there are still not many numerically accurate techniques which can be used to solve it even for the simplest case of 1D problem. Certainly, there are several implementations of Monte-Carlo [6,7] and adding-doubling [8,9] codes which allow one to make a simulation with high accuracy. However, they are not efficient in the case when it is necessary to know the radiance characteristics at all points and in all directions within the scattering medium. In the latter case only the vector discrete ordinate radiative transfer model (VDOM) [10–13] and the generalized spherical harmonics approximation (GSHA) [14,15] may be suggested to choose from. These two techniques have derived from their scalar analogs: the discrete ordinate method (DOM) and spherical harmonics approximation (SHA). Case and Zweifel [16] show that taking into account that the DOM is based on the Gaussian quadrature formula there is a close relationship between the DOM and the version of SHA. The major difference between these two methods results from the fact that a regular DOM implementation employs for all azimuthal harmonics the same Gaussian quadrature formula which is the most accurate for the zeroth harmonic. As discussed by Karp and Petrack [17] this formula generates the larger error the higher the order of the azimuthal harmonic which is calculated. Similar arguments can be used in comparison of the VDOM and GSHA and should be taken into account when a numerical technique to simulate the polarization characteristics of the radiance propagated in scattering and absorbing media is required.

The main goal of this paper is to develop a computationally efficient technique to simulate polarized radiative transfer through a stratified slab, which additionally provides the ability to estimate the perturbation integrals [18]. We believe that the GSHA should be chosen since it allows us to estimate these perturbation integrals analytically.

The GSHA as a direct descendent of the SHA inherits similar drawbacks. The first of them follows from the fact that within the framework of the GSHA the radiance is represented as a finite series of the generalized spherical functions. It leads to the impossibility to meet the boundary conditions exactly, and as a consequence it results in unavoidable oscillations at regions near a boundary.

To overcome this problem in the SHA a few techniques have been suggested [19–21], but from our point of view a method based on iteration of the radiative transfer solution is an optimal one. From the computational point of view it is not the fastest technique, but it provides the highest overall accuracy.

The next difficulty is a consequence of the fact that aerosols and clouds may consist of rather large particles. Hence, to represent the phase function of such a medium as a series of Legendre polynomials with a reasonable accuracy one has to take into account several hundred polynomials. Most of them are essential in order to describe the diffraction peak accurately. To make a problem easier following the results of [22] we may consider the radiance as consisting of two components: the first one (usually called a small-angle component) is propagated near the direction of illumination and generated by the presence of the diffraction peak. The second component is responsible for description of radiance at angles which are larger than the diffraction peak width. As it was shown [22] that these two components can be considered independent with high accuracy and hence different methods can be used to calculate them. Moreover, if there is no interest to simulate the radiance within that small-angle region, the diffraction peak can be cut off and considered as a part of the unscattered light. This technique as applied to polarized light propagation was used by Zege et al [23].

The paper is organized as follows. Section 2 introduces the basic notations which are necessary to describe the polarized radiative transfer problem based on the Stokes-vector framework in the complex representation. The derivation of the vector radiative transfer equation using a variational principle is discussed in Section 3 together with derivation of the corresponding approximations. Possible methods to represent the boundary condition in the discrete form are also considered in Section 3. Section 4 is devoted to consideration of how one can make the computational process more efficient. The Appendix contains the necessary information regarding to the properties of the generalized spherical functions.

2 Definitions

To characterize both the energy and polarization properties of light at the depth z in the direction \vec{n} the Stokes vector $\mathbf{I} = (I, Q, U, V)^T$ is generally used (T means the matrix transposition operation). Because the components of the Stokes vector do not constitute a vector in the strict geometrical sense, its definition relates strongly to the choice of coordinate system and which direction of rotation is defined as positive. Some discussion of this problem can be found in [24]. Our definition is the same as Chandrasekhar's [4,24].

The polarization characteristics of the radiance are determined by the polarization state of the source which is sometimes inconvenient since it increases the number of parameters to explore in simulations. This is important for the perturbation calculation [18] which usually requires one to solve the vector radiative transfer equation (VRTE) for the same geometry but assuming sources with different polarization states. It can be done more efficiently by employing a matrix technique which allows one to find a solution of the VRTE regardless the polarization characteristics of the source by introduction of the matrix, $\mathbf{G}(z, \vec{n})$, defined by

$$\mathbf{I}(z, \vec{n}) = \mathbf{G}(z, \vec{n})\mathbf{i}_0, \quad (1)$$

where \mathbf{i}_0 is the Stokes vector of the source radiance normalized to the intensity, I . We will Since $\mathbf{G}(z, \vec{n})$ allows us to find a solution of for arbitrary polarization sater This makes our problem completely independent of the polarization state of the source: however it increases slightly the computational load in comparison to simulations when only a single polarization state of the source is required.

The most widely used representation of the Stokes vector in the form $\mathbf{I} = (I, Q, U, V)^T$, however, is not the only possibility. In this paper we shall use the so called complex representation of the Stokes vector,

$$\mathbf{I}_c = \frac{1}{2}(Q - iU, I - V, I + V, Q + iU)^T, \quad (2)$$

which has an advantage of having simple properties upon rotating the coordinate system (more details can be found in [24]). We shall distinguish between the representations by using the 'c' subscript for all quantities in the complex representation. The transition from the energetic to complex representations can be written in the form

$$\mathbf{I}_c = \mathbf{A}\mathbf{I}, \quad (3)$$

where

$$\mathbf{A} = \frac{1}{2} \begin{pmatrix} 0 & 1 & i & 0 \\ 1 & 0 & 0 & 1 \\ 1 & 0 & 0 & -1 \\ 0 & 1 & -i & 0 \end{pmatrix}. \quad (4)$$

For the sake of simplicity, we assume that our medium can be represented as a composition of N homogeneous slabs. We shall use the Cartesian system with the origin situated on the medium boundary and z -axis directed along the inner normal into the medium, while the xz -plane coincides with the plane of incidence. The direction \vec{n} is characterized by the zenith angle, θ , and the azimuth angle, ϕ , which are measured from the z -axis and xz -plane, respectively. The optical properties of the medium are as usual characterized by

the extinction coefficient, σ_e , the scattering coefficient, σ_s , and the scattering matrix, $\mathbf{P}(\cos \beta)$ (here β is the scattering angle).

3 Variational Principle and Vector Radiative Transfer Equation

In our pursuit to find an approximate solution for the VRTE we shall employ the variational technique suggested in [25] and start with the functional

$$\begin{aligned}
F = & \int_0^H \int_{4\pi} [\tilde{\mathbf{I}}^+(z, \vec{n}) \hat{\mathbf{L}} \mathbf{I}(z, \vec{n}) + \tilde{\mathbf{I}}^+(z, \vec{n}) \mathbf{S}_c + \mathbf{R}_c^+ \mathbf{I}(z, \vec{n})] d\vec{n} dz \\
& - \int_{\mu < 0} \tilde{\mathbf{I}}^+(H, \vec{n}) \left[\mathbf{I}(H, \vec{n}) - \frac{1}{\pi} \int_{\mu' > 0} \mathbf{M}_c(\vec{n}, \vec{n}') \mathbf{I}(H, \vec{n}') \mu' d\vec{n}' \right] \mu d\vec{n} \\
& + \int_{\mu > 0} \tilde{\mathbf{I}}^+(0, \vec{n}) \mathbf{I}(0, \vec{n}) \mu d\vec{n}. \quad (5)
\end{aligned}$$

Here (+) means the Hermitian conjugation operation introduced for compatibility between the energetic and complex representations, and

$$\hat{\mathbf{L}} = \mu \frac{d}{dz} + \sigma_e(z) - \frac{\sigma_s(z)}{4\pi} \int_{4\pi} d\vec{n}' \mathbf{Z}(z, \vec{n}, \vec{n}') \otimes, \quad (6)$$

where \otimes means that the last term is an integral operator and not a simple integral. $\tilde{\mathbf{I}}$ is a vector, the physical meaning of which will be explained later.

$\mathbf{Z}(z, \vec{n}, \vec{n}')$ is the phase matrix. As discussed by Chandrasekhar [4] the phase matrix is related to the scattering matrix $\mathbf{P}(z, \cos \beta)$ by

$$\mathbf{Z}(z, \vec{n}, \vec{n}') = \mathbf{L}(\pi - \chi_1) \mathbf{P}(z, \cos \beta) \mathbf{L}(-\chi_2). \quad (7)$$

$\mathbf{L}(\chi)$ is the matrix which is required to rotate a meridian plane through angles $\pi - \chi_1$ and $-\chi_2$ before and after scattering onto the local scattering plane (the angles system is shown on Fig. 1).

\mathbf{S} and \mathbf{R} represent the source and receiver functions and have the form

$$\mathbf{S} = \mathbf{s}_0 S(z, \vec{n}), \quad (8)$$

$$\mathbf{R} = \mathbf{r}_0 R(z, \vec{n}), \quad (9)$$

where \mathbf{s}_0 and \mathbf{r}_0 describe the source and receiver polarization states, and the scalar functions, $S(z, \vec{n})$ and $R(z, \vec{n})$, describe the sources in the medium and the receiver function, respectively.

$\mathbf{M}(\vec{n}, \vec{n}')$ determines the reflection properties of the underlying surface. In the simplest case of the Lambertian model, $\mathbf{M}(\vec{n}, \vec{n}')$ has the form

$$\mathbf{M}(\vec{n}, \vec{n}') = \begin{pmatrix} A & 0 & 0 & 0 \\ 0 & 0 & 0 & 0 \\ 0 & 0 & 0 & 0 \\ 0 & 0 & 0 & 0 \end{pmatrix}. \quad (10)$$

Here A is the coefficient for Lambertian reflection (albedo).

By taking a variational derivative of (5) over $\tilde{\mathbf{I}}$, the VRTE with the corresponding boundary conditions which governs \mathbf{I} can be derived in the form similar to one introduced by Chandrasekhar [4] for the Stokes vector:

$$\left[\mu \frac{d}{dz} + \sigma_e(z) \right] \mathbf{I}(z, \vec{n}) = \frac{\sigma_s(z)}{4\pi} \int_{4\pi} \mathbf{Z}(z, \vec{n}, \vec{n}') \mathbf{I}(z, \vec{n}) d\vec{n}' + \mathbf{S}(z, \vec{n}), \quad (11)$$

$$\mathbf{I}(0, \vec{n}) = 0, \quad \text{if } \mu > 0; \quad (12a)$$

$$\mathbf{I}(H, \vec{n}) = \frac{1}{\pi} \int_{\mu' > 0} \mathbf{M}(\vec{n}, \vec{n}') \mathbf{I}(H, \vec{n}') \mu' d\vec{n}', \quad \text{if } \mu < 0. \quad (12b)$$

Moreover, if we calculate the functional derivative over \mathbf{I} we obtain an equation which shall be solved to calculate the adjoint function $\tilde{\mathbf{I}}$ and has the form:

$$\left[-\mu \frac{d}{dz} + \sigma_e(z) \right] \tilde{\mathbf{I}}(z, \vec{n}) = \frac{\sigma_s(z)}{4\pi} \int_{4\pi} \mathbf{Z}^+(z, \vec{n}', \vec{n}) \tilde{\mathbf{I}}(z, \vec{n}') d\vec{n}' + \mathbf{R}(z, \vec{n}) \quad (13)$$

with the boundary conditions:

$$\tilde{\mathbf{I}}(0, \vec{n}) = 0, \quad \text{if } \mu < 0, \quad (14a)$$

$$\tilde{\mathbf{I}}(H, \vec{n}) = \frac{1}{\pi} \int_{\mu' < 0} \mathbf{M}^+(\vec{n}', \vec{n}) \tilde{\mathbf{I}}(H, \vec{n}') \mu' d\vec{n}', \quad \text{if } \mu > 0. \quad (14b)$$

Recalling the reciprocity principle (see for example [26])

$$\mathbf{Z}^+(z, -\vec{n}, -\vec{n}') = \mathbf{T} \mathbf{Z}^+(z, \vec{n}', \vec{n}) \mathbf{T}, \quad (15)$$

where (+) denotes the Hermitian conjugation operation (used instead of transposition for compatibility with the complex representation),

$$\mathbf{T} = \text{diag}[1, 1, -1, 1]. \quad (16)$$

Comparing Eqs. (11) and (13) it can be noticed that if

$$R(z, \vec{n}) = S(z, -\vec{n}) \quad (17)$$

then

$$\tilde{\mathbf{I}}(z, \vec{n}) = \mathbf{T}\mathbf{I}(z, -\vec{n})\mathbf{T}. \quad (18)$$

Thus, $\tilde{\mathbf{I}}$ is a consequence of the reciprocity of the Maxwell's equations for the electromagnetic field and represents a solution which backtracks the photons detected by the receiver back to the source. There is no difference as to which equations to solve, only the convenience of implementation has to be taken into account.

Functional (5) provides a natural way to derive an approximation to calculate \mathbf{I} by approximating the integral. For all cases a convenient starting point is to represent all essential quantities of Eq. (5) in the form of series over the azimuthal harmonics:

$$\mathbf{I} = \sum_{m=-M}^M \mathbf{I}^m \exp(-im\phi), \quad (19a)$$

$$\tilde{\mathbf{I}} = \sum_{m=-M}^M \tilde{\mathbf{I}}^m \exp(-im\phi), \quad (19b)$$

$$R = \sum_{m=-M}^M R^m \exp(-im\phi), \quad (19c)$$

$$S = \sum_{m=-M}^M S^m \exp(-im\phi), \quad (19d)$$

$$\mathbf{Z} = \sum_{m=-M}^M \mathbf{Z}^m \exp(-im\phi). \quad (19e)$$

We can choose to derive a finite-difference approximation for the integral [27] by providing the corresponding functions at points μ_k and then to calculate the variational derivative over $\tilde{\mathbf{I}}^m(z, \mu_k)$. Recalling the orthogonality of the azimuthal harmonics we may immediately write the discrete ordinate approximation of the VRTE in the form:

$$\left[\mu_k \frac{d}{dz} + \sigma_e(z) \right] \mathbf{I}^m(z, \mu_k) = \frac{\sigma_s(z)}{4\pi} \sum_{j=1}^N w_j \mathbf{Z}^m(z, \mu_k, \mu_j) \mathbf{I}^m(z, \mu_j) + R^m(z, \mu_k) \quad (20)$$

with the approximate boundary conditions:

$$\mathbf{I}^m(0, \mu_k) = 0, \quad \text{for } \mu_k > 0, \quad (21a)$$

$$\mathbf{I}^m(H, \mu_k) = \frac{1}{\pi} \sum_{\mu_j > 0} w_j \mathbf{M}^m(\mu_k, \mu_j) \mathbf{I}^m(H, \mu_j) \mu_j, \quad \text{for } \mu_k < 0. \quad (21b)$$

Here w_j are the weights which are used in the Gaussian type [27, Ch. 25] integration formulas. For instance, the VDOM [12] employs the Gauss integration formula with the corresponding choice of the abscissas μ_k and the weights w_k .

Another possibility can be explored if the complex representation of the corresponding functions is being used. Let us represent the quantities listed in Eq. (19) as series over the generalized spherical harmonics:

$$\mathbf{I}_c^m(z, \mu) = \sum_{l=0}^N (2l+1) \mathbf{Y}_m^l(\mu) \mathbf{f}_m^l, \quad (22a)$$

$$\tilde{\mathbf{I}}_c^m(z, \mu) = \sum_{l=0}^N (2l+1) \mathbf{Y}_m^l(\mu) \tilde{\mathbf{f}}_m^l, \quad (22b)$$

$$\mathbf{R}_c^m = \sum_{l=0}^N (2l+1) \mathbf{Y}_m^l(\mu) \mathbf{r}_m^l, \quad (22c)$$

$$\mathbf{S}_c^m = \sum_{l=0}^N (2l+1) \mathbf{Y}_m^l(\mu) \mathbf{s}_m^l, \quad (22d)$$

where \mathbf{f}_m^l and $\tilde{\mathbf{f}}_m^l$ are complex vectors which are also functions of z , z_0 and \vec{n}_0 , but we assume this dependence implicitly to simplify the notation. The matrix, $\mathbf{Y}_m^l(\mu)$, has the diagonal form

$$\mathbf{Y}_m^l(x) = \text{diag}[P_{2,m}^l(x), P_{0,m}^l(x), P_{-0,m}^l(x), P_{-2,m}^l(x)]. \quad (23)$$

Some selected properties of the polynomials $P_{0,m}^l(x)$ can be found in Appendix A. As it was demonstrated the coefficients of the representation of the phase matrix in [24] do not depend on the azimuthal harmonic index, m ,

$$\mathbf{Z}_c^m(\mu, \mu') = \sum_{l=0}^N (2l+1) \mathbf{Y}_m^l(\mu) \mathbf{g}^l \mathbf{Y}_m^l(\mu'). \quad (24)$$

The variational derivative over $\tilde{\mathbf{f}}_m^l$ with consequent integration over μ and ϕ gives us the full set of equations to determine \mathbf{f}_m^l :

$$\mathbf{A}_m^l \frac{d}{dz} \mathbf{f}_m^{l-1} + \mathbf{B}_m^l \frac{d}{dz} \mathbf{f}_m^l + \mathbf{A}_m^{l+1} \frac{d}{dz} \mathbf{f}_m^{l+1} + (2l+1) [\sigma_e(z) \mathbf{E} - \sigma_s(z) \mathbf{g}^l] \mathbf{f}_m^l = \mathbf{r}_m^l \quad (25)$$

with a clear assumption that $\mathbf{f}_m^l = 0$ for $l < |m|$ since $\mathbf{Y}_m^l(\mu) = 0$ for $l < |m|$. Here \mathbf{E} is the 4-by-4 identity matrix. To make this system finite we set that

$$\mathbf{f}_m^l = 0, \quad \text{for } l \geq N_m, \quad (26)$$

where N_m is usually chosen even by the similar reasons as discussed by Case and Zweifel [16] for the scalar case. Thus, we obtain an approximate solution

for \mathbf{I}_c as

$$\mathbf{I}_c(z, \vec{n}) = \sum_{m=-M}^M \sum_{l=|m|}^{N_m-1} (-1)^m (2l+1) \exp(im\phi) \mathbf{Y}_m^l(\mu) \mathbf{f}_m^l, \quad (27)$$

Following Dave[19] we define $N_m = N_0 - |m| + \text{mod}(N_0 - |m|, 2)$, where the function $\text{mod}(x_1, x_2)$ returns the remainder when the first argument, x_1 , is divided by the second argument, x_2 .

The boundary conditions are obtained in the form:

$$\int_{\mu>0} e^{is\phi} \mathbf{Y}_m^{|m|+k}(\mu) \mathbf{G}_c(0, \vec{n}) d\vec{n} = 0, \quad (28a)$$

$$\int_{\mu<0} e^{is\phi} \mathbf{Y}_m^{|m|+k}(\mu) \mathbf{G}_c(H, \vec{n}) d\vec{n} = \frac{1}{\pi} \int_{\mu<0} \int_{\mu'>0} e^{is\phi} \mathbf{Y}_m^{|m|+k}(\mu) \mathbf{M}_c(\vec{n}, \vec{n}') \mathbf{G}_c(H, \vec{n}') \mu' d\vec{n}' d\vec{n}, \quad (28b)$$

where $-M \leq m \leq M$ and $0 \leq k < N_m$. As is clearly seen, the total number of the boundary conditions is $2N_m$, which is two times more than is necessary. In the scalar case employing the symmetry of the associated Legendre polynomials [27] it can be demonstrated that only odd moments have to be chosen as boundary conditions [28,29] (see also footnote #2 in [30]). Unfortunately, the generalized spherical functions do not have such nice symmetry properties which made it unsuccessful for us to derive the Marshak type boundary conditions from the variational principle. However, keeping the equivalence between the scalar case and our problem we postulate that boundary conditions in the form of Eq. (28) are valid only if $k = 1, 3, \dots, N_m - 1$.

In the most general case Eq. (28) requires joint solution of Eqs. (25) and (28) for all azimuthal harmonics at the same time. However, the generally accepted assumption that the surface reflection matrix depends only on $\phi - \phi'$ allows one to consider every azimuthal harmonic of the Stokes matrix independently and, thus, to simplify the computation process dramatically. Introducing

$$\mathbf{M}_c^m(\mu, \mu') = \frac{1}{2\pi} \int_0^{2\pi} e^{im(\phi-\phi')} \mathbf{M}_c(\vec{n}, \vec{n}') d\phi \quad (29)$$

and substituting (27) into (28b) we readily obtain

$$\sum_{l=|s|}^{N_s^l} (2l+1) \Phi_m^{s,k,l} [\mathbf{f}_s^l(H)]_m = 2 \sum_{l=|s|}^{N_s^l} (2l+1) \sum_k \Psi_{m,k}^{s,k,l} [\mathbf{f}_s^l(H)]_k, \quad (30)$$

where

$$\Phi_{n,m}^{k,l} = \int_{-1}^0 P_{n,m}^{n+2k+1}(\mu) P_{n,m}^l(\mu) d\mu \quad (31a)$$

$$\Psi_{m,k}^{s,k,l} = \int_{-1}^0 \int_0^1 P_{s,m}^{s+2k+1}(\mu) [\mathbf{M}_s(\mu, \mu')]_{m,k} P_{s,k}^l(\mu') \mu' d\mu' d\mu \quad (31b)$$

and the indexes m and k run through $[+2, +0, -0, -2]$ and the notation $[\mathbf{f}_s^l(H)]_m$ underlines that we use the m th component of the vector \mathbf{f}_s^l at depth $z = H$. $\Phi_{n,m}^{k,l}$ can be calculated analytically (see Appendix C), however, an analytical expression for $\Psi_{m,k}^{s,k,l}$ can be obtained only in selected cases (for example, for a Lambertian underlying surface).

Equations (25) and (30) provide us with a full equation set to determine the coefficient $\mathbf{f}_s^l(z)$ and, hence, the Stokes vector employing Eq. (27). One can always combine Eq. (25) with the Mark type boundary conditions (21) with an appropriate choice of the quadrature formula (see for example [15]).

4 Calculation Technique

In the previous section we have considered derivation of the generalized spherical harmonics approximation of the VRTE with the corresponding approximate boundary conditions. However, the direct implementation of the derived formulas is not the most efficient way to make a simulation. There are a few factors which should be considered in order to increase computational efficiency. The most noticeable is that the total radiation is a mixture of the direct and scattered components. Clearly, this is of importance in the case of directed sources such as the Sun radiation. We may also need to handle the phase function peak and to estimate the effect of the source polarization state on the measurement result.

4.1 Direct radiation

Separate treatment of the direct and scattered components of the radiation is a commonly used technique which allows one to increase significantly the computational accuracy in the case of directional sources. It is based on the radiance representation in the form of

$$\mathbf{I}(z, \mu) = \mathbf{I}_s(z, \mu) + \mathbf{I}_0(z, \mu), \quad (32)$$

where in the case of solar illumination

$$\mathbf{I}_0(z, \mu) = \mathbf{i}_0 \exp(-\tau/\mu_0) \delta(\vec{n} - \vec{n}_0) \quad (33)$$

where $\mathbf{i}_0 = [1, 0, 0, 0]^T$, $\tau = \int_0^z \sigma_e(t) dt$ is the optical thickness, \vec{n}_0 is the direction of the solar illumination and μ_0 is its cosine. $\mathbf{I}_s(z, \mu)$ satisfies the same VRTE (11) with the corresponding modifications introduced into the source term and boundary conditions. For the solar illumination it has the form

$$\left[\mu \frac{d}{dz} + \sigma_e(z) \right] \mathbf{I}_s(z, \vec{n}) = \frac{\sigma_s(z)}{4\pi} \int_{4\pi} \mathbf{Z}(z, \vec{n}, \vec{n}') \mathbf{I}_s(z, \vec{n}') d\vec{n}', \\ + \frac{\sigma_s(z)}{4\pi} \mathbf{Z}(z, \vec{n}, \vec{n}_0) \mathbf{i}_0 \exp(-\tau/\mu_0), \quad (34)$$

and

$$\mathbf{I}_s(0, \vec{n}) = 0, \quad \text{if } \mu > 0; \quad (35a)$$

$$\mathbf{I}_s(H, \vec{n}) = \frac{1}{\pi} \int_{\mu' > 0} \mathbf{M}(\vec{n}, \vec{n}') [\mathbf{I}_s(H, \vec{n}') + \mathbf{I}_0(H, \vec{n}')] \mu' d\vec{n}', \quad \text{if } \mu < 0. \quad (35b)$$

4.2 Treatment of the phase function peak

The scattering matrix for the clouds, and aerosols such as dust or sea salt, contains hundreds of terms in the decomposition into the generalized spherical function series. This feature usually results in increasing demands for computational time and/ or processor power. However, the large number of terms is a consequence of the scattering matrix having a pronounced peak in the small angle region. Accounting for this peak is essential only for a limited number of problems which require an accurate calculation in the vicinity to the direction of the illumination. For many problems (for example, satellite observation modeling) this information is of a little importance and, thus, a δ -Eddington-like technique can be implemented.

In the scalar case the conventional treatment of the peak is splitting the phase function into two parts - the peak and the rest of the phase function, the later we shall call diffusive. Then, the peak is modeled as a δ -function. This procedure assumes implicitly that the part of the phase function which is considered as the peak must have the average cosine close to 1.0 and a non negligible weight. The former requirement is clear if one takes into account the results of the asymptotic theory which considers the average cosine of the phase function as the most important characteristic of the phase function which in many cases determines the properties of the reflected and transmitted radiance in the asymptotic regime [31]. However, a straightforward application of this

technique for the polarized transfer could be dangerous since the elements of the scattering matrix have different functional dependencies on the scattering angle. It is known that the polarization characteristics of the scattered radiance (at least in the first order scattering approximation) depend on the ratio between the corresponding elements of the scattering matrix. Thus, to preserve these ratios one may use a technique suggested by Zege et al. [23] which relies on the scattering matrix representation in the form

$$\mathbf{P} = p \mathbf{P}_n, \quad (36)$$

where p is the phase function and \mathbf{P}_n is the matrix which consists of the elements of the scattering matrix normalized on p . Let p can be represented as

$$p = a_p p_p + a_d p_d, \quad (37)$$

where p_p and p_d have the same normalization as the phase function and represent the peak and diffusive parts of the phase function, respectively; a_p and a_d are constants such that

$$a_p + a_d = 1.0. \quad (38)$$

Substituting (37) into (36) we obtain a splitting algorithm for the scattering matrix in the form

$$\mathbf{P} = a_p \mathbf{P}_p + a_d \mathbf{P}_d \quad (39)$$

where clearly

$$\mathbf{P}_p = p_p \mathbf{P}_n, \quad \mathbf{P}_d = p_d \mathbf{P}_n.$$

Employing the idea of the multicomponent approach [22] the solution of Eq. (11) can be represented as a sum

$$\mathbf{I}_s = \mathbf{I}_p + \mathbf{I}_d, \quad (40)$$

where in the case of solar illumination

$$\begin{aligned} \left[\mu \frac{d}{dz} + \sigma_e \right] \mathbf{I}_p(z, \vec{n}) &= a_p \frac{\sigma_s}{4\pi} \int_{4\pi} \mathbf{Z}_p(\vec{n}, \vec{n}') \mathbf{I}_p(z, \vec{n}') d\vec{n}' \\ &\quad + a_p \frac{\sigma_s(z)}{4\pi} \mathbf{Z}_p(z, \vec{n}, \vec{n}_0) \mathbf{i}_0 \exp(-\tau/\mu_0), \end{aligned} \quad (41a)$$

$$\begin{aligned} \left[\mu \frac{d}{dz} + (\sigma_e - a_p \sigma_s) \right] \mathbf{I}_d(z, \vec{n}) &= \frac{\sigma_s}{4\pi} \int_{4\pi} a_d \mathbf{Z}_d(\vec{n}, \vec{n}') \mathbf{I}_d(z, \vec{n}') d\vec{n}' \\ &\quad + a_d \frac{\sigma_s}{4\pi} \int_{4\pi} \mathbf{Z}_d(\vec{n}, \vec{n}') [\mathbf{I}_p(z, \vec{n}') + \mathbf{I}_0(z, \vec{n}')] d\vec{n}'. \end{aligned} \quad (41b)$$

In the equation for $\mathbf{I}_d(z, \vec{n})$ we have made the assumption that the angular width of the peak phase function is negligible in comparison with that of p_d and, thus, it may be replaced by a δ -function.

At this stage we can neglect the contribution of the component $\mathbf{I}_p(z, \vec{n})$, which can be made for all directions except those close to direction of the initial

illumination. In this case we should solve (41.a) assuming that

$$\mathbf{P}_p = \mathbf{E}\delta(\vec{n} - \vec{n}'), \quad (42)$$

which is equivalent to the δ -Eddington approximation. Another way to avoid an expensive numerical calculation is to solve (41.a) approximately using the small-angle approximation. The later technique provides estimations of the \mathbf{I}_p which are accurate enough for many applications as we shall demonstrate below.

According to the framework of the small angle approximation [32,33], μ in the differential operator of (41.a) is replaced with μ_0 . If

$$\mathbf{I}_p(z, \vec{n}) = \sum_{m=-M}^M \sum_{l=|m|}^{N_m-1} (-1)^m (2l+1) \exp(im\phi) \mathbf{Y}_m^l(\mu) \mathbf{f}_m^l, \quad (43)$$

then, taking into account the orthogonality of \mathbf{Y}_s^l we have

$$\mu_0 \frac{d\mathbf{f}_m^l}{dz} + [\sigma_e(z) - a_p \sigma_s(z) \mathbf{g}_p^l] \mathbf{f}_m^l = a_p \frac{\sigma_s(z)}{4\pi} \mathbf{g}_p^l \mathbf{Y}_m^l(\mu_0) \mathbf{i}_0 \exp(-\tau/\mu_0). \quad (44)$$

In the case of $\mu_0 > 0$ and assuming homogeneity of the scattering medium, the solution has the form

$$\mathbf{f}_s^l = \left[\exp\left(-[\sigma_e \mathbf{E} - a_p \sigma_s \mathbf{g}_p^l] z/\mu_0\right) - \exp(-\sigma_e \mathbf{E} z/\mu_0) \right] \mathbf{Y}_m^l(\mu_0) \frac{\mathbf{i}_0}{4\pi\mu_0}, \quad (45)$$

where the matrix exponent has been used.

The form of the coefficient dependence allows us to make a further simplification. Namely, we can perform summation on the azimuth harmonics for a given l analytically employing the addition theorem, Eq. (A.5). As a result, we can write

$$\mathbf{I}_p(z, \vec{n}) = \sum_{l=0}^{N_m-1} (-1)^m (2l+1) \mathbf{L}(\pi - \chi_1^0) \mathbf{J}^l \mathbf{L}(\chi_2^0) \frac{\mathbf{i}_0}{4\pi\mu_0}, \quad (46)$$

where

$$\mathbf{J}^l|_{qp} = \left[\exp\left(-[\sigma_e \mathbf{E} - a_p \sigma_s \mathbf{g}_p^l] z/\mu_0\right) - \exp(-\sigma_e \mathbf{E} z/\mu_0) \right] |_{qp} P_{pq}^l(\mu'). \quad (47)$$

Here p and q denote the component indexes of the 4-by-4 matrix and can be $+2, +0, -0, -2$. μ' and angles χ_1^0 and χ_2^0 are determined similar to the way they are defined in the phase matrix definition, Eq. (7), using the directions \vec{n}_0 and \vec{n} .

4.3 Source polarization state

Another factor which may increase the computational burden is the necessity to study how a given measurement result depends on the polarization state of the source which occurs in perturbation calculations [18]. Traditionally, to be able to solve this problem one has to make simulations for four different polarization states of the source. However, using the matrix formalism (1) rather than Stokes vector and its symmetry properties one can reduce significantly the amount of the required calculation as we shall demonstrate.

This matrix can be introduced because of linearity of the VRTE. For the scattering component of the radiation we may write

$$\mathbf{I}_s(z, \vec{n}) = \mathbf{G}_s(z, \vec{n}) \mathbf{i}_0 \quad (48)$$

which allows us to rewrite (34) in the form

$$\left[\mu \frac{d}{dz} + \sigma_e(z) \right] \mathbf{G}_s(z, \vec{n}) = \frac{\sigma_s(z)}{4\pi} \int_{4\pi} \mathbf{Z}(z, \vec{n}, \vec{n}') \mathbf{G}_s(z, \vec{n}') d\vec{n}' + \frac{\sigma_s(z)}{4\pi} \mathbf{Z}(z, \vec{n}, \vec{n}_0) \exp(-\tau/\mu_0). \quad (49)$$

Since \mathbf{i}_0 is an arbitrary vector it can be canceled in the both right and left hand sides of the equation. The boundary conditions take the form

$$\mathbf{G}_s(0, \vec{n}) = 0, \quad \text{if } \mu > 0; \quad (50a)$$

$$\mathbf{G}_s(H, \vec{n}) = \frac{1}{\pi} \int_{\mu' > 0} \mathbf{M}(\vec{n}, \vec{n}') [\mathbf{G}_s(H, \vec{n}') + \mathbf{G}_0(H, \vec{n}')] \mu' d\vec{n}', \quad \text{if } \mu < 0, \quad (50b)$$

where

$$\mathbf{G}_0(z, \vec{n}) = \mathbf{E} \exp(-\tau/\mu_0) \delta(\vec{n} - \vec{n}_0). \quad (51)$$

Similar to the expansion of \mathbf{I} into the general harmonic series (27) we can expand \mathbf{G} as (assuming the complex representation)

$$\mathbf{G}_c(z, \vec{n}) = \sum_{m=-M}^M \sum_{l=|m|}^{N_m-1} (-1)^m (2l+1) \exp(im\phi) \mathbf{Y}_m^l(\mu) \mathbf{h}_m^l, \quad (52)$$

where in the case of solar illumination the matrices \mathbf{h}_m^l satisfy the equation

$$\mathbf{A}_m^l \frac{d}{dz} \mathbf{h}_m^{l-1} + \mathbf{B}_m^l \frac{d}{dz} \mathbf{h}_m^l + \mathbf{A}_m^{l+1} \frac{d}{dz} \mathbf{h}_m^{l+1} + (2l+1) [\sigma_e(z) \mathbf{E} - \sigma_s(z) \mathbf{g}^l] \mathbf{h}_m^l = a_p \frac{\sigma_s(z)}{4\pi} \mathbf{g}^l \exp(-\tau/\mu_0) \quad (53)$$

and the corresponding boundary conditions. This equation allows us to deduce the symmetry properties of the matrices \mathbf{h}_m^l which reduces the amount of required calculations.

4.4 Symmetry properties of \mathbf{h}_s^l

The first can be deduced from the fact that the scattering matrix, \mathbf{F} , is real

$$\mathbf{F}(\cos \beta) = \overline{\mathbf{F}}(\cos \beta). \quad (54)$$

Here \bar{x} denotes the complex conjugation of x . Hence, in the complex representation, we can write that

$$\overline{\mathbf{F}}_c(\cos \beta) = \mathbf{T} \mathbf{F}_c(\cos \beta) \mathbf{T}, \quad (55)$$

where

$$\mathbf{T} = \begin{pmatrix} 0 & 0 & 0 & 1 \\ 0 & 1 & 0 & 0 \\ 0 & 0 & 1 & 0 \\ 1 & 0 & 0 & 0 \end{pmatrix}, \quad (56)$$

and $\mathbf{T} \mathbf{T} = \mathbf{E}$.

From Eq.(55) and the properties of the generalized spherical function (Appendix A) a similar relationship follows for the expansion coefficient of the scattering matrix (B.7),

$$\overline{\mathbf{g}}^l = \mathbf{T} \mathbf{g}^l \mathbf{T}. \quad (57)$$

Let both sides of Eq.(53) be left- and right- multiplied by \mathbf{T} , and then complex conjugated. Taking into account the obvious relationships

$$\mathbf{T} \mathbf{A}_m^l \mathbf{T} = \mathbf{A}_m^l = \mathbf{A}_{-m}^l, \quad \overline{\mathbf{A}}_m^l = \mathbf{A}_m^l \quad (58a)$$

$$\mathbf{T} \mathbf{B}_m^l \mathbf{T} = \mathbf{B}_{-m}^l, \quad \overline{\mathbf{B}}_m^l = \mathbf{B}_m^l \quad (58b)$$

$$\mathbf{T} \mathbf{Y}_m^l \mathbf{T} = \mathbf{Y}_{-m}^l, \quad \overline{\mathbf{Y}}_m^l = (-1)^s \mathbf{Y}_m^l \quad (58c)$$

we obtain

$$\begin{aligned} \mathbf{A}_m^l \frac{d}{dz} \mathbf{T} \overline{\mathbf{h}}_{-m}^{l-1} \mathbf{T} + \mathbf{B}_m^l \frac{d}{dz} \mathbf{T} \overline{\mathbf{h}}_{-m}^l \mathbf{T} + \mathbf{A}_m^{l+1} \frac{d}{dz} \mathbf{T} \overline{\mathbf{h}}_{-m}^{l+1}(x) \mathbf{T} + \\ \left[(2l+1)\sigma_e(z)\mathbf{E} - \sigma_s(z)\mathbf{g}^l \right] \mathbf{T} \overline{\mathbf{f}}_{-m}^l \mathbf{T} = \\ = (-1)^m \frac{\sigma_s(z)}{4\pi} \exp(im\phi_0) \mathbf{g}^l \mathbf{Y}_m^l(\mu_0) \exp(-\tau/\mu_0) \end{aligned} \quad (59)$$

Comparing with Eq.(25) we conclude that

$$\mathbf{f}_{-m}^l = (-1)^m \mathbf{T} \bar{\mathbf{f}}_m^l \mathbf{T} \quad (60)$$

and we have to calculate only \mathbf{f}_m^l for $m \geq 0$ to obtain the final solution.

Another symmetry relationship can be derived taking into account that [24]

$$\mathbf{F}_c(\cos \beta) = \mathbf{Q} \mathbf{F}_c(\cos \beta) \mathbf{Q}, \quad (61)$$

where

$$\mathbf{Q} = \begin{pmatrix} 0 & 0 & 0 & 1 \\ 0 & 0 & 1 & 0 \\ 0 & 1 & 0 & 0 \\ 1 & 0 & 0 & 0 \end{pmatrix}, \quad (62)$$

and analogously

$$\mathbf{g}^l = \mathbf{Q} \mathbf{g}^l \mathbf{Q}. \quad (63)$$

Applying transformation \mathbf{Q} to Eq.(25) and taking into account the obvious identities

$$\mathbf{Q} \mathbf{A}_m^l \mathbf{Q} = \mathbf{A}_m^l = \mathbf{A}_{-m}^l \quad (64a)$$

$$\mathbf{Q} \mathbf{B}_m^l \mathbf{Q} = \mathbf{B}_{-m}^l \quad (64b)$$

$$\mathbf{Q} \mathbf{Y}_m^l \mathbf{Q} = \mathbf{Y}_{-m}^l \quad (64c)$$

and then comparing the result with Eq.(25) we readily obtain

$$\mathbf{f}_{-m}^l = \mathbf{Q} \mathbf{f}_m^l \mathbf{Q}. \quad (65)$$

Substitution of (60) into (65) provides us with

$$\mathbf{f}_m^l = (-1)^m \mathbf{T} \mathbf{Q} \bar{\mathbf{f}}_m^l \mathbf{Q} \mathbf{T}, \quad (66)$$

which means that the third column of \mathbf{f}_m^l is related to the second column as

$$\begin{pmatrix} [\mathbf{f}_m^l]_{+2,+0} \\ [\mathbf{f}_m^l]_{+0,+0} \\ [\mathbf{f}_m^l]_{-0,+0} \\ [\mathbf{f}_m^l]_{-2,+0} \end{pmatrix} = (-1)^m \begin{pmatrix} [\bar{\mathbf{f}}_m^l]_{+2,-0} \\ [\bar{\mathbf{f}}_m^l]_{-0,-0} \\ [\bar{\mathbf{f}}_m^l]_{+0,-0} \\ [\bar{\mathbf{f}}_m^l]_{-2,-0} \end{pmatrix} \quad (67)$$

As a cumulative result of the use of Eqs.(60, 67) the amount of calculation is reduced approximately by a factor of three in comparison to a straightforward implementation, which makes this technique competitive with the direct calculation of the Stokes vector.

4.5 Simulation

To verify our code we made simulations for numerous cases available (e.g [14,10,34,35]); however, here, for the sake of space, we will demonstrate only results relevant to the $L = 13$ task suggested by Garcia and Siewert [14]. The problem is to determine Stokes parameters of the radiation propagated through the homogeneous cloud of the optical thickness 1.0 illuminated by the Sun and situated over a Lambertian underlying surface with albedo of 0.1. The cosine of the Sun angle is 0.2. The scattering matrixes were calculated using "Greek" constants taken from [36] and listed in Table 1. Note that for this particular problem a sum of the first 10 azimuthal harmonics provides more than sufficient accuracy.

The results of our simulations with parameters $N_0=400$ are depicted in Tables 2, and 3. They agree with data tabulated by Garcia and Siewert [14,10] with the accuracy up to the last digit (in most cases) while the time required to perform these simulations was enormous. As a rule, such an accuracy (6 digits) is rarely needed. Since the generalized spherical harmonic approximation does not allow one to have the computational accuracy estimation, we performed simulations using several values of N_0 . Selected results are depicted in Tables 4 and 5. These tables provide us with an answer to the question - how many terms in Eq. (22a) should be taken into account to achieve a given accuracy of computation.

Table 4 shows that even the value N_0 of 20 provides the intensity estimation with the relative error of 0.5%. The accuracy better than 0.1% can be obtained if the simulations are conducted with $N_0 \geq 40$. Computation of the polarization characteristics (Q , U , and V) usually requires more accurate simulations. For example, to achieve the relative error $\sim 1.0\%$ for Q estimation, including points where Q changes the sign and, thus, can be extremely small (e.g. $Q(\tau = 0.75, \mu = -0.4, \phi - \phi_0 = 0) = -3.0068910^{-4}$), simulations have to be performed with $N_0 \geq 80$ (see Table 5). These points are usually situated near neutral (unpolarized) points where $Q = 0$. Moreover, to achieve the relative error $\sim 0.1\%$ of Q calculation $N_0 \geq 200$ must be chosen. However, if the polarization characteristics near neutral points is not of special interest, the simulation with $N_0 \geq 40$ is enough to achieve accuracy better than 0.1%.

The goal of our next simulation is to demonstrate that the use of the small angle approximation can be successfully used to treat the phase function peak as discussed in Section 4.2. We shall use as an example the problem of solar radiation propagation through a homogeneous cloud. The optical properties of the cloud are described by Deirmendjian cloud model Cloud C.1. at $0.550 \mu\text{m}$ [37]. The optical thickness of the cloud is 1.0. To describe accurately the scattering matrix it is required to include more than 200 terms in decomposi-

tion (24). However, if the phase function peak is cut at the level of 10° , only 20 terms can successfully describe the diffusive part of the phase function (Fig. 2). Figure 3 demonstrates how the removal of the peak changes the value of the corresponding coefficients.

Figure 4 depicts the radiance distribution at the level $\tau = 0.5$ inside the cloud calculated using two approaches. The first used the full scattering matrix and the Stokes vector was represented as the sum, Eq. (27), with $M = 2$ and $N_0 = 200$ and the results are shown by the solid lines. The second one used the small angle approximation to treat the peak and to calculate the diffusive part $N_0 = 20$ was used. Its results are depicted by the cross symbols. The figure shows that the accuracy of such an approach is excellent while the computational time required is more than 10 times less for the second approach.

5 Conclusion

We demonstrated that the generalized spherical harmonics approximation as well as the vector discrete ordinate method can be obtained with the use of the variational principle. Thus, we established the basis for the equivalence for these two approaches and we may state that their accuracy depends on how accurately they approximate the integral of the functional in (5). The variational principle used allowed us to derive the approximate boundary conditions. However, in contrast to the scalar case the Marshak type boundary conditions cannot be validated since the symmetry properties of the generalized spherical function are different from the associated Legendre polynomials. This makes the Marshak type boundary conditions less accurate than the Mark ones.

The overall accuracy of the generalized spherical harmonics approximation cannot be estimated without more accurate calculations similar to the scalar case. However, the suggested approach based on removing the scattering matrix peak allows one to use only limited number of polynomials (our practice shows that 20 is enough) while keeping the accuracy of the calculations at a reasonable level. Assuming the uncertainty of the optical properties of the atmosphere such an accuracy level seems to us to be a fair trade for computational speed and efficiency. Moreover, one may neglect the suggested use of the small angle approximation if there is no interest in the radiance distribution at the angles close to the direction of the initial propagation.

Acknowledgments. This work was supported by the Australian Research Council A39917202.

A Properties of the generalized spherical functions $P_{nm}^l(x)$

In this appendix the most important properties of the generalized spherical function are presented. The more detailed information can be found in [38,39], where they are considered through their connection to a rotation group.

For integers n, m, l with $l \geq \max(|n|, |m|)$ the generalized spherical functions may be defined in the form

$$P_{mn}^l(x) = (-1)^{l-n} \frac{i^{n-m}}{2^l} \sqrt{\frac{(l+m)!}{(l-n)!(l+n)!(l-m)!}} \\ \times (1+x)^{-\frac{n+m}{2}} (1-x)^{\frac{n-m}{2}} \frac{d^{l-m}}{dx^{l-m}} \left[(1-x)^{l-n} (1+x)^{l+n} \right]. \quad (\text{A.1})$$

They are a solution of the differential equation

$$(1-x^2) \frac{d^2}{dx^2} P_{nm}^l - 2x \frac{d}{dx} P_{nm}^l + \left[l(l+1) - \frac{m^2 + n^2 - 2mnx}{1-x^2} \right] P_{nm}^l = 0. \quad (\text{A.2})$$

The generalized spherical functions are orthogonal with respect to the upper index

$$\int_{-1}^1 P_{mn}^l(x) P_{nm}^k(x) dx = \frac{2}{2l+1} (-1)^{n+m} \delta_{lk}. \quad (\text{A.3})$$

and functions $\sqrt{l+0.5} P_{nm}^l(x)$ for $l = \max(|m|, |n|), \dots, \infty$ constitute a complete orthonormal system on $[-1, +1]$ with the inner product

$$\langle f, g \rangle = \int_{-1}^1 \bar{f} g dx, \quad (\text{A.4})$$

where \bar{f} denotes the complex conjugation of f .

The generalized spherical functions satisfy the addition theorem

$$e^{im\chi_1} P_{mn}^l(\cos \beta) e^{in\chi_2} = \sum_{s=-l}^l (-1)^s e^{is(\phi-\phi')} P_{ms}^l(\cos \theta) P_{sn}^l(\cos \theta'). \quad (\text{A.5})$$

Here the angles β, χ_1, χ_2 and the directions $\vec{n} = (\theta, \phi)$ and $\vec{n}' = (\theta', \phi')$ are the same as in relationship (7) between the phase and scattering matrices.

The generalized spherical functions are symmetric with respect to several operations with the indexes n and m

$$P_{mn}^l(x) = P_{nm}^l(x) = P_{-m, -n}^l(x) \quad (\text{A.6})$$

and have the parity relation

$$P_{mn}^l(-x) = (-1)^{l+m-n} P_{-m,n}^l(x). \quad (\text{A.7})$$

The complex conjugation of $P_{mn}^l(x)$ leads to

$$\overline{P_{mn}^l(x)} = (-1)^{m-n} P_{mn}^l(x). \quad (\text{A.8})$$

The generalized spherical function can be calculated directly using the formula

$$P_{mn}^l(x) = i^{-n-m} \sqrt{\frac{(l-m)!(l-n)!}{(l+m)!(l+n)!}} \left(\frac{1+x}{1-x}\right)^{\frac{m+n}{2}} \times \sum_{j=\max(m,n)}^l \frac{(-1)^j (l+j)!}{(l-j)!(j-m)!(j-n)!} \left[\frac{1-x}{2}\right]^j \quad (\text{A.9})$$

or the recurrence relations

$$(2l+1) \left[x - \frac{mn}{l(l+1)} \right] P_{m,n}^l(x) = \alpha_{mn}^{l+1} P_{m,n}^{l+1}(x) + \alpha_{nm}^l P_{n,m}^{l-1}(x), \quad (\text{A.10})$$

with the initialization

$$P_{ln}^l(x) = \frac{i^{l-n}}{2^l} \sqrt{\frac{(2l)!}{(l+n)!(l-n)!}} (1+x)^{\frac{l+n}{2}} (1-x)^{\frac{l-n}{2}}, \quad (\text{A.11})$$

$$P_{ln}^{l-1}(x) = 0, \quad (\text{A.12})$$

where

$$\alpha_{mn}^l = \frac{\sqrt{(l^2-n^2)(l^2-m^2)}}{l} \quad (\text{A.13})$$

Most of the properties of the generalized spherical functions can be derived employing their relationship to the hypergeometric function [27]

$$P_{nm}^l(x) = \frac{(-i)^{n-m}}{2^n(n-m)!} \sqrt{\frac{(l-m)!(l+n)!}{(l+m)!(l-n)!}} (1-x)^{\frac{n-m}{2}} (1+x)^{\frac{n+m}{2}} \times F\left(-l+n, l+n+1; n-m+1; \frac{1-x}{2}\right), \quad (\text{A.14})$$

$$= \frac{(-1)^{l-m} i^{n-m}}{2^n(n+m)!} \sqrt{\frac{(l+m)!(l+n)!}{(l-m)!(l-n)!}} (1-x)^{\frac{n-m}{2}} (1+x)^{\frac{n+m}{2}} \times F\left(-l+n, l+n+1; n+m+1; \frac{1+x}{2}\right). \quad (\text{A.15})$$

In particular, with the help of the Gauss relations one can obtain the fol-

lowing recurrence relationships:

$$i\sqrt{1-x^2}P_{m,n+1}^l(x) = \sqrt{\frac{l+1+n}{l-n}} \left[x - \frac{m}{l+1} \right] P_{m,n}^l(x) - \frac{\alpha_{mn}^{l+1}}{\sqrt{l-n}} P_{n,m}^{l+1}(x), \quad (\text{A.16})$$

$$2i \frac{n-mx}{\sqrt{1-x^2}} P_{nm}^l(x) = \sqrt{(l-m+1)(l+m)} P_{n,m-1}^l(x) - \sqrt{(l+m+1)(l-m)} P_{n,m+1}^l(x), \quad (\text{A.17})$$

$$(1-x^2) \frac{dP_{m,n}^l(x)}{dx} = \alpha_{mn}^l P_{m,n}^{l-1}(x) - \left[lx - \frac{nm}{l} \right] P_{n,m}^l(x), \quad (\text{A.18})$$

$$\frac{d}{dx} P_{nm}^l(x) = \frac{m-nx}{1-x^2} P_{nm}^l(x) + i \sqrt{\frac{(l-n)(l+n+1)}{(1-x^2)}} P_{n+1,m}^l(x) \quad (\text{A.19})$$

B Properties of the matrix \mathbf{Y}_m^l

The convenience of the matrix \mathbf{Y}_s^l becomes clear from consideration of relationship (7) between the phase and scattering matrices. Let the explicit form of the scattering matrix in the complex representation be represented as

$$\mathbf{P}_c(z, \cos \beta) = \begin{pmatrix} a_{+2,+2} & a_{+2,+0} & a_{+2,-0} & a_{+2,-2} \\ a_{+0,+2} & a_{+0,+0} & a_{+0,-0} & a_{+0,-2} \\ a_{-0,+2} & a_{-0,+0} & a_{-0,-0} & a_{-0,-2} \\ a_{-2,+2} & a_{-2,+0} & a_{-2,-0} & a_{-2,-2} \end{pmatrix}. \quad (\text{B.1})$$

Then substituting the explicit form of the rotation matrix $\mathbf{L}_c(\chi)$,

$$\mathbf{L}_c(\chi) = \text{diag}[\exp(-i2\chi), 1, 1, \exp(i2\chi)], \quad (\text{B.2})$$

into (7) the corresponding components of the phase matrix may be written as

$$[\mathbf{Z}_c(z, \vec{n}, \vec{n}')]_{m,n} = e^{im\chi_1} a_{m,n} e^{in\chi_2}. \quad (\text{B.3})$$

Here the indexes n and m run through $[+2, +0, -0, -2]$.

Let $a_{m,n}$ may be decomposed into a series of the generalized spherical functions

$P_{nm}^l(x)$ as

$$a_{m,n} = \sum_{\max(|m|,|n|)}^{\infty} (2l+1)g_{m,n}^l P_{m,n}^l. \quad (\text{B.4})$$

Now, addition theorem (A.5) allows us to obtain a series for the components of the phase matrix

$$\begin{aligned} [\mathbf{Z}_c(z, \vec{n}, \vec{n}')]_{m,n} = \\ \sum_{\max(|m|,|n|)}^{\infty} \sum_{s=-l}^l (2l+1)(-1)^s \exp[i s(\phi - \phi')] P_{s,m}^l(\cos \theta) g_{m,n}^l P_{n,s}^l(\cos \theta'). \end{aligned} \quad (\text{B.5})$$

This formula provides the basic reason to introduce a diagonal matrix \mathbf{Y}_s^l constructed from the generalized spherical function as

$$\mathbf{Y}_s^l(x) = \text{diag}[P_{2,s}^l(x), P_{0,s}^l(x), P_{-0,s}^l(x), P_{-2,s}^l(x)] \quad (\text{B.6})$$

which allows us to rewrite (B.5) using the matrix notation

$$\mathbf{Z}_c(z, \vec{n}, \vec{n}') = \sum_{l=0}^{\infty} \sum_{s=-l}^l (2l+1)(-1)^s \exp[i s(\phi - \phi')] \mathbf{Y}_s^l(\cos \theta) \mathbf{g}^l \mathbf{Y}_s^l(\cos \theta') \quad (\text{B.7})$$

having assumed that $[\mathbf{g}^l]_{m,n} = g_{m,n}^l$, $g_{m,n}^l = 0.0$ for $0 \leq l < \max(|m|, |n|)$. This decomposition makes it possible to develop the generalized spherical harmonics approximation, the computational aspects of which have been considered in this paper.

To conclude the discussion of \mathbf{Y}_s^l , it is useful to write down the recurrence relationship for \mathbf{Y}_s^l , which is a simple generalization of (A.10) and has the form

$$(2l+1) [x - \mathbf{B}_s^l] \mathbf{Y}_s^l = \mathbf{A}_s^{l+1} \mathbf{Y}_s^{l+1} + \mathbf{A}_s^l \mathbf{Y}_s^l(x), \quad (\text{B.8})$$

where

$$\mathbf{A}_s^l = \text{diag}[\alpha_{2,s}^l(x), \alpha_{0,s}^l(x), \alpha_{-0,s}^l(x), \alpha_{-2,s}^l(x)], \quad (\text{B.9})$$

$$\mathbf{B}_s^l = \frac{s}{l(l+1)} \text{diag}[2, 0, 0, -2]. \quad (\text{B.10})$$

C Integrals

We are interested in calculation of the integral

$$\int_a^b P_{nm}^l(x) P_{nm}^k(x) dx \quad (\text{C.1})$$

Taking into account Eq.(A.2) we obtain

$$\frac{d}{dx}(1-x^2)\frac{d}{dx}P_{nm}^l = - \left[l(l+1) - \frac{m^2 + n^2 - 2mnx}{1-x^2} \right] P_{nm}^l$$

and

$$\begin{aligned} P_{nm}^k \frac{d}{dx}(1-x^2)\frac{d}{dx}P_{nm}^l - P_{nm}^l \frac{d}{dx}(1-x^2)\frac{d}{dx}P_{nm}^k \\ = \frac{d}{dx}(1-x^2) \left[P_{nm}^k \frac{d}{dx}P_{nm}^l - P_{nm}^l \frac{d}{dx}P_{nm}^k \right] \\ = (k-l)(l+k+1)P_{nm}^l P_{nm}^k, \end{aligned}$$

which provides us with the integral

$$\begin{aligned} \int_a^b P_{nm}^l(x)P_{nm}^k(x)dx &= \frac{(1-x^2)}{(k-l)(l+k+1)} \left[P_{nm}^k \frac{d}{dx}P_{nm}^l - P_{nm}^l \frac{d}{dx}P_{nm}^k \right] \Big|_a^b \\ &= \frac{i\sqrt{1-x^2}}{(k-l)(l+k+1)} \left[\sqrt{(l-n)(l+n+1)}P_{nm}^k P_{n+1,m}^l(x) \right. \\ &\quad \left. - \sqrt{(k-n)(k+n+1)}P_{nm}^l P_{n+1,m}^k(x) \right] \Big|_a^b \\ &= \frac{\alpha_{mn}^l P_{nm}^k P_{nm}^{l-1} - \alpha_{mn}^k P_{nm}^l P_{nm}^{k-1}}{(k-l)(l+k+1)} + \frac{1}{k+l+1} \left[x + \frac{nm}{kl} \right] P_{nm}^l P_{nm}^k \Big|_a^b \end{aligned}$$

If $a = -1$ and $b = 1$ taking into account that

$$P_{nm}^l(-1) = \begin{cases} 0, & n \neq -m, \\ (-1)^l, & n = -m \end{cases},$$

$$P_{nm}^l(1) = \begin{cases} 0, & n \neq m, \\ 1, & n = m \end{cases}.$$

we have

$$\int_{-1}^1 P_{nm}^l(x)P_{nm}^k(x)dx = 0, \quad \text{for } l \neq k. \quad (\text{C.2})$$

To estimate the integral for $k = l$ we consider

$$(1 - x^2) P_{nm}^l \frac{dP_{nm}^{l+1}(x)}{dx} = \alpha_{nm}^{l+1} P_{nm}^l P_{nm}^l(x) - \left[(l+1)x - \frac{nm}{l+1} \right] P_{nm}^l P_{nm}^{l+1}, \quad (\text{C.3})$$

$$(1 - x^2) P_{nm}^{l+1} \frac{dP_{nm}^l(x)}{dx} = \left[(l+1)x - \frac{nm}{l+1} \right] P_{nm}^{l+1} P_{nm}^l(x) - \alpha_{nm}^{l+1} P_{nm}^{l+1} P_{nm}^{l+1}(x) \quad (\text{C.4})$$

which provides us with

$$(1 - x^2) \frac{dP_{nm}^{l+1} P_{nm}^l}{dx} = \alpha_{nm}^{l+1} P_{nm}^l P_{nm}^l(x) - \alpha_{nm}^{l+1} P_{nm}^{l+1} P_{nm}^{l+1}(x) \quad (\text{C.5})$$

or

$$\frac{d(1 - x^2) P_{nm}^{l+1} P_{nm}^l}{dx} = \alpha_{nm}^{l+1} P_{nm}^l P_{nm}^l(x) - \alpha_{nm}^{l+1} P_{nm}^{l+1} P_{nm}^{l+1}(x) - 2x P_{nm}^{l+1} P_{nm}^l. \quad (\text{C.6})$$

The use of the recurrence relationship results in

$$\begin{aligned} \frac{d(1 - x^2) P_{nm}^{l+1} P_{nm}^l}{dx} &= \alpha_{nm}^{l+1} \left[P_{nm}^l P_{nm}^l(x) - \frac{2l+3}{2l+1} P_{nm}^{l+1} P_{nm}^{l+1} \right] - \\ &\quad \frac{2a_{nm}^l}{2l+1} P_{nm}^{l-1} P_{nm}^{l+1} - \frac{nm}{l(l+1)} P_{nm}^l P_{nm}^{l+1} \quad (\text{C.7}) \end{aligned}$$

and, finally,

$$\begin{aligned} \int_a^b P_{nm}^{l+1} P_{nm}^{l+1} dx &= \frac{2l+1}{2l+3} \int_a^b P_{nm}^l P_{nm}^l(x) dx - \frac{2a_{nm}^l}{(2l+3)\alpha_{nm}^{l+1}} \int_a^b P_{nm}^{l-1} P_{nm}^{l+1} dx - \\ &\quad \frac{1}{\alpha_{nm}^{l+1}} \frac{2l+1}{2l+3} \left[\frac{nm}{l(l+1)} \int_a^b P_{nm}^l P_{nm}^{l+1} dx + (1 - x^2) P_{nm}^{l+1} P_{nm}^l \Big|_a^b \right]. \quad (\text{C.8}) \end{aligned}$$

To initialize the recurrence in the case of $a = 0$ and $b = 1$ we can use the following

$$\int_0^1 P_{0l}^l(x) P_{0l}^l(x) dx = \frac{(-1)^l}{2l+1}, \quad (\text{C.9})$$

$$\int_0^1 P_{\pm 1l}^l(x) P_{\pm 1l}^l(x) dx = -(-1)^l \left(\frac{1}{2l+1} \pm \frac{2^{-2l}(2l)!}{l!(l+1)!} \right), \quad (\text{C.10})$$

$$\int_0^1 P_{\pm 2l}^l(x) P_{\pm 2l}^l(x) dx = (-1)^l \left(\frac{1}{2l+1} \pm \frac{2^{1-2l}(2l)!}{(l+2)(l!)^2} \right). \quad (\text{C.11})$$

References

- [1] Mischenko MI, Travis LD. Satellite retrieval of aerosol properties over the ocean using polarization as well as intensity of reflected sunlight. *J. Geophys. Res.* 1997;102:16989–17013.
- [2] Leroy M, Deuze JL, Breon FM, Hautecoeur O, Herman M, Buriez JC, Tanre D, Bouffies S, Chazette P, Roujean JL. Retrieval of atmospheric properties and surface bidirectional reflectances over land from POLDER/ADEOS. *J. Geophys. Res.* 1997;102:17023–17037.
- [3] Chang PCY, Walker JG, Hopcraft KI, Ablitt B, Jakeman E. Polarization discrimination for active imaging in scattering media. *Opt. Comm.* 1999;159:1–6.
- [4] Chandrasekhar S. Radiative transfer. New York:Oxford University Press, 1950.
- [5] Rozenberg GV. Stokes vector-parameter. *Uspekhi Fiz. Nauk* 1955;51:76–110.
- [6] Marchuk G, Mikhailov G, Nazarlijev M, Darbinjan R, Kargin B, Elepov B. The Monte-Carlo methods in atmospheric optics. Heidelberg:Springer-Verlag, 1980.
- [7] Tynes HH, Kattawar GW, Zege EP, Katsev IL, Prikhach AS, Chaikovskaya LI. Monte carlo and multicomponent approximation methods for vector radiative transfer by use of effective mueller matrix calculations. *Appl. Optics* 2001;40:400–412.
- [8] Wauben WMF, de Haan JF, Hovenier JW. A method for computing visible and infrared polarized monochromatic radiation in planetary atmospheres. *Astron. Astrophys* 1994;282:277–290.
- [9] Hovenier JW, Domke H, Mee CVM van der. Transfer of polarized light in planetary atmospheres: Basic concepts and practical methods (Astrophysics and space science library, v. 318). Dordrecht:Kluwer, 2004.
- [10] Garcia RDM, Siewert CE. The F_N method for radiative transfer models that include polarization effects. *J. Quant. Spectrosc. Radiat. Transfer* 1989;41:117–145.
- [11] Evans KF, Stephens GL. A new polarized atmospheric radiative transfer model. *J. Quant. Spect. Rad. Transfer* 1991;46:413–423.
- [12] Schulz FM, Stammes K, Weng F. VDISORT: an improved and generalized discrete ordinate radiative transfer model for polarized (vector) radiative transfer computations. *J. Quant. Spectrosc. Radiat. Transfer* 1999;61:105–122.
- [13] Qin Y, Box MA. Vector Green’s function algorithm for radiative transfer in plane-parallel atmosphere. *J. Quant. Spect. Rad. Transfer* 2006;97:228–251.
- [14] Garcia RDM, Siewert CE. A generalized spherical harmonics solution for radiative transfer models that include polarization effects. *J. Quant. Spectrosc. Radiat. Transfer* 1986;36:401–423.

- [15] Ustinov EA. Method of spherical harmonics: application to the transfer of polarized light in vertically nonuniform planetary atmosphere. *Mathematical apparatus. Kosmicheskie Issledovaniya* 1988;26:473–484.
- [16] Case KM, Zweifel PF. *Linear transport theory*. Massachusetts: Addison-Wesley, 1967.
- [17] Karp AH, Petrack S. On the spherical harmonics and discrete ordinates methods for azimuth-dependent intensity calculations. *J. Quant. Spectrosc. Radiat. Transfer* 1982;30:161–165.
- [18] Polonsky IN, Box MA. General perturbation technique for the calculation of radiative effects in scattering and absorbing media. *J. Opt. Soc. Amer. A* 2002;19:2281–2292.
- [19] Dave JV. A direct solution of the spherical harmonics approximation to the radiative equation for an arbitrary solar elevation. Part I: Theory. *J. Atmos. Sci.* 1975;32:790–7989.
- [20] Takeuchi Y. Use of spherical harmonics in the solution of the radiation transfer problem. *J. Quant. Spectrosc. Radiat. Transfer* 1988;39:237–245.
- [21] Lyapustin AI, Muldashev TZ. Method of spherical harmonics in the radiative transfer problem with non-lambertian surface. *J. Quant. Spectrosc. Radiat. Transfer*. 1999;61:545–555.
- [22] Zege EP, Katsev IL, Polonsky IN. Multicomponent approach to light propagation in clouds and mists. *Appl. Opt.* 1993;32:2803–2812.
- [23] Zege EP, Katsev IL, Prikhach AS, Chaikovskaya LI. Private communication 2002.
- [24] Hovenier JW, Mee CVM van der. Fundamental relationships relevant to the transfer of polarized light in a scattering atmosphere. *Astron. Astrophys.* 1983;128:1–16.
- [25] Pomraning GC. A variational principle for linear systems. *J. Soc. Indust. Appl. Math.* 1965;13:511–519.
- [26] Mischenko MI, Hovenier JW, Travis LD (Eds). *Light Scattering by Nonspherical Particles. Theory, Measurements and Applications*. San-Diego: Academic, 2000.
- [27] Abramowitz M, Stegun IA (Eds). *Handbook of Mathematical Functions with Formulas, Graphs, and Mathematical Tables*. 1980.
- [28] Davis JA. Variational vacuum boundary conditions for a P_N approximation. *Nucl. Sci. Eng.* 1966;25:189–197.
- [29] Vladimirov VS. Mathematical problems in the one-velocity theory of particle transport. Tech. Rep. Tech. Rep. AECL-1661. Atomic Energy of Canada Ltd., Chalk River, Ontario (1963).
- [30] Marshak R.E. Note on the spherical harmonic method as applied to the milne problem for a sphere. *Phys. Rev.* 1947;71:43–43.

- [31] Zege EP, Ivanov AP, Katsev IL. Image transfer through a scattering medium. Heidelberg:Springer-Verlag, 1991.
- [32] Bremmer H. Random volume scattering. Radio Sci. 1964;D68:967–981.
- [33] Dolin L, Levin I. Undewater optics. in: Encyclopedia of Applied Physics. Vol. 12. VCH Publishers, 1995. pp. 571–601.
- [34] Siewert CE. A concise and accurate solution for a polarization model in radiative transfer. J. Quant. Spect. Rad. Transfer 1999;62:677–684.
- [35] Siewert CE. A discrete-ordinates solution for radiative-transfer models that include polarization elects. J. Quant. Spect. Rad. Transfer 2000;64:227–254.
- [36] Vestrucci P, Siewert CE. A numerical evaluation of an analytical representation of the components in a fourier decomposition of the phase matrix for the scattering of polarized light. J. Quant. Spect. Rad. Transfer 1984;31:177–183.
- [37] Deirmendjian D. Electromagnetic scattering on spherical polydispersions. New York:American Elsevier Pub. Co., 1969.
- [38] Gelfand IM, Mintos RA, Shapiro ZYa. Representations of the rotation and Lorentz groups and their applications. New York:Macmillan, 1963.
- [39] Vilenkin NJa. Special functions and the theory of group representation. Providence:America Mathematical Society, 1968.

List of Tables

- 1 The "Greek" constants used in the simulation and taken from [36].
- 2 The Stokes parameter $I(\tau, \mu, \phi - \phi_0 = 0)$ for the $L = 13$ problem.
- 3 The Stokes parameter $Q(\tau, \mu, \phi - \phi_0 = 0)$ for the $L = 13$ problem.
- 4 Relative error [in percent] of estimation of the Stokes parameter $I(\tau, \mu, \phi - \phi_0 = 0)$ for the $L = 13$ problem. The results of the simulation with $N_0=400$ are assumed of being exact.
- 5 Relative error [in percent] of estimation of the Stokes parameter $Q(\tau, \mu, \phi - \phi_0 = 0)$ for the $L = 13$ problem. The results of the simulation with $N_0=400$ are assumed of being exact.

Table 1

The "Greek" constants used in the simulation and taken from [36].

β	α	ζ	δ	γ	ϵ
1.0	0.0	0.0	0.7120634246	0.0	0.0
1.4552931819	0.0	0.0	1.7601411931	0.0	0.0
1.0540263128	3.3091220464	2.5773207443	1.0668243107	-0.7552491518	0.0420726875
0.3975899378	0.9633758276	0.7574437604	0.3965110389	-0.3619934319	0.0850671555
0.1165930161	0.2474124256	0.1638155665	0.0957641237	-0.1155748816	0.0154318420
0.0238747702	0.0452636955	0.0278314781	0.0176508810	-0.0249815879	0.0031534874
0.0039501033	0.0068892608	0.0038897148	0.0026154886	-0.0041675362	0.0004010299
0.0005388807	0.0008798202	0.0004642654	0.0003271332	-0.0005739043	0.0000460147
0.0000637172	0.0000987255	0.0000490224	0.0000358314	-0.0000677900	0.0000042875
0.0000066697	0.0000099029	0.0000046647	0.0000035142	-0.0000070926	0.0000003617
0.0000006329	0.0000009071	0.0000004075	0.0000003148	-0.0000006712	0.0000000272
0.0000000553	0.0000000769	0.0000000331	0.0000000261	-0.0000000585	0.0000000019
0.0000000045	0.0000000061	0.0000000025	0.0000000020	-0.0000000047	0.0000000001
0.0000000003	0.0000000005	0.0000000002	0.0000000001	-0.0000000004	0.0000000000

Table 2

The Stokes parameter $I(\tau, \mu, \phi - \phi_0 = 0)$ for the $L = 13$ problem.

μ	τ					
	0.0	0.1	0.2	0.5	0.75	1.0
-1.0	5.49562e-02	4.33456e-02	3.47492e-02	1.95907e-02	1.28199e-02	8.74689e-03
-0.8	1.25600e-01	9.22140e-02	6.87258e-02	3.15055e-02	1.71322e-02	8.74689e-03
-0.6	2.19341e-01	1.57805e-01	1.15037e-01	4.90474e-02	2.41484e-02	8.74689e-03
-0.4	3.62679e-01	2.58220e-01	1.86227e-01	7.74889e-02	3.68020e-02	8.74689e-03
-0.2	6.02870e-01	4.25516e-01	3.04077e-01	1.26933e-01	6.36364e-02	8.74689e-03
0.0	1.11633e+00	7.92854e-01	5.54307e-01	2.16684e-01	1.19875e-01	6.94685e-02
0.2	0.00000e+00	3.77196e-01	4.93653e-01	3.64182e-01	2.20559e-01	1.33508e-01
0.4	0.00000e+00	2.00959e-01	2.98791e-01	3.18324e-01	2.49366e-01	1.83224e-01
0.6	0.00000e+00	1.18553e-01	1.85496e-01	2.32658e-01	2.08977e-01	1.74764e-01
0.8	0.00000e+00	6.53705e-02	1.05917e-01	1.48705e-01	1.47069e-01	1.35062e-01
1.0	0.00000e+00	1.83910e-02	3.18366e-02	5.42516e-02	6.22532e-02	6.53175e-02

Table 3

The Stokes parameter $Q(\tau, \mu, \phi - \phi_0 = 0)$ for the $L = 13$ problem.

μ	τ					
	0.0	0.1	0.2	0.5	0.75	1.0
-1.0	-2.16087e-02	-1.44003e-02	-9.66518e-03	-3.04102e-03	-1.01472e-03	0.00000e+00
-0.8	-3.50476e-02	-2.28372e-02	-1.50735e-02	-4.71193e-03	-1.68885e-03	0.00000e+00
-0.6	-3.27677e-02	-2.02041e-02	-1.26615e-02	-3.57485e-03	-1.37406e-03	0.00000e+00
-0.4	-2.27545e-02	-1.17143e-02	-5.85401e-03	-5.58396e-04	-3.00689e-04	0.00000e+00
-0.2	-6.64319e-03	2.28629e-03	5.58723e-03	5.15000e-03	2.24298e-03	0.00000e+00
0.0	-8.04672e-04	1.69088e-02	1.99133e-02	1.42873e-02	8.33816e-03	2.50381e-03
0.2	0.00000e+00	8.06383e-03	1.49468e-02	1.93034e-02	1.45868e-02	8.82210e-03
0.4	0.00000e+00	8.63773e-04	3.78697e-03	1.01383e-02	1.06072e-02	8.54149e-03
0.6	0.00000e+00	-5.56101e-03	-6.96560e-03	-3.83085e-03	-9.79789e-04	2.78039e-04
0.8	0.00000e+00	-1.04497e-02	-1.55948e-02	-1.75331e-02	-1.47868e-02	-1.20241e-02
1.0	0.00000e+00	-1.06100e-02	-1.71824e-02	-2.45081e-02	-2.48012e-02	-2.34396e-02

Table 4

Relative error [in percent] of estimation of the Stokes parameter $I(\tau, \mu, \phi - \phi_0 = 0)$ for the $L = 13$ problem. The results of the simulation with $N_0=400$ are assumed of being exact.

μ	N_0	τ					
		0.0	0.1	0.2	0.5	0.75	1.0
-1.0	20	-0.3412	-0.1506	-0.1494	-0.3022	-0.3409	-0.1988
	40	-0.0877	-0.0378	-0.0570	-0.0730	-0.0811	-0.0529
	80	-0.0215	-0.0125	-0.0141	-0.0179	-0.0195	-0.0129
	200	-0.0027	-0.0016	-0.0017	-0.0026	-0.0023	-0.0016
-0.4	20	-0.3706	-0.0341	0.0161	-0.2469	-0.4182	-0.1988
	40	-0.0957	-0.0015	-0.0306	-0.0537	-0.0867	-0.0529
	80	-0.0234	-0.0062	-0.0081	-0.0132	-0.0215	-0.0129
	200	-0.0030	-0.0008	-0.0011	-0.0015	-0.0027	-0.0016
0.4	20	0.0000	-0.6439	-0.3702	-0.1583	-0.1672	-0.2309
	40	0.0000	-0.1582	-0.0716	-0.0484	-0.0469	-0.0600
	80	0.0000	-0.0299	-0.0181	-0.0119	-0.0116	-0.0147
	200	0.0000	-0.0035	-0.0023	-0.0016	-0.0016	-0.0022
1.0	20	0.0000	-0.7210	-0.4668	-0.2732	-0.2631	-0.2814
	40	0.0000	-0.1838	-0.0996	-0.0734	-0.0697	-0.0729
	80	0.0000	-0.0370	-0.0242	-0.0179	-0.0172	-0.0178
	200	0.0000	-0.0043	-0.0031	-0.0024	-0.0022	-0.0021

Table 5

Relative error [in percent] of estimation of the Stokes parameter $Q(\tau, \mu, \phi - \phi_0 = 0)$ for the $L = 13$ problem. The results of the simulation with $N_0=400$ are assumed of being exact.

μ	N_0	τ					
		0.0	0.1	0.2	0.5	0.75	1.0
-1.0	20	-0.1647	0.0111	0.0387	-0.1197	-0.2188	0.0000
	40	-0.0430	0.0049	-0.0108	-0.0214	-0.0424	0.0000
	80	-0.0106	-0.0021	-0.0028	-0.0053	-0.0108	0.0000
	200	-0.0014	0.0000	-0.0003	-0.0007	-0.0010	0.0000
-0.4	20	1.0829	0.3022	-0.0473	5.7692	9.7024	0.0000
	40	0.2597	0.0367	0.1780	1.2590	1.7496	0.0000
	80	0.0615	0.0282	0.0482	0.3005	0.4210	0.0000
	200	0.0075	0.0034	0.0056	0.0371	0.0519	0.0000
0.4	20	0.0000	-31.0530	-6.5377	-1.1244	-0.8409	-1.0680
	40	0.0000	-7.4090	-1.2194	-0.3354	-0.2338	-0.2720
	80	0.0000	-1.3974	-0.2960	-0.0809	-0.0566	-0.0663
	200	0.0000	-0.1726	-0.0372	-0.0099	-0.0066	-0.0082
1.0	20	0.0000	-0.3393	-0.2002	-0.1016	-0.0992	-0.1041
	40	0.0000	-0.0858	-0.0419	-0.0294	-0.0274	-0.0282
	80	0.0000	-0.0170	-0.0105	-0.0073	-0.0069	-0.0073
	200	0.0000	-0.0019	-0.0012	-0.0008	-0.0008	-0.0009

List of Figures

- 1 Geometry of a scattering event. The direction of the incident light is \vec{n}_1 while the scattered light one is \vec{n}_2 ($0 \leq \phi_1 \leq \phi_2 \leq \pi$).
- 2 Phase function of the cloud model Cloud C1 at $0.55 \mu\text{m}$ (solid line) and its diffusion component (dashed line).
- 3 Coefficients of the decomposition of the phase function (dots) and its diffusion component (crosses) into Legendre polynomials.
- 4 Component of the Stokes vector I and the ratio Q/I as the function of the observational angle, θ at the level of $\tau = 0.5$. Scattering properties are described by the Deirmendjian cloud model Cloud C.1. at $0.550 \mu\text{m}$. Single scattering albedo is assumed to be 0.95. The total optical thickness of the cloud is 1.0. Sunlight illumination at $\mu_0 = 1.0$. Solid line depicts the accurate simulation results using 200 polynomials and 2 azimuthal harmonics while symbols show results obtained with the use of the small angle approximation and the generalized spherical harmonics calculation using only 20 polynomials and 2 azimuthal harmonics.

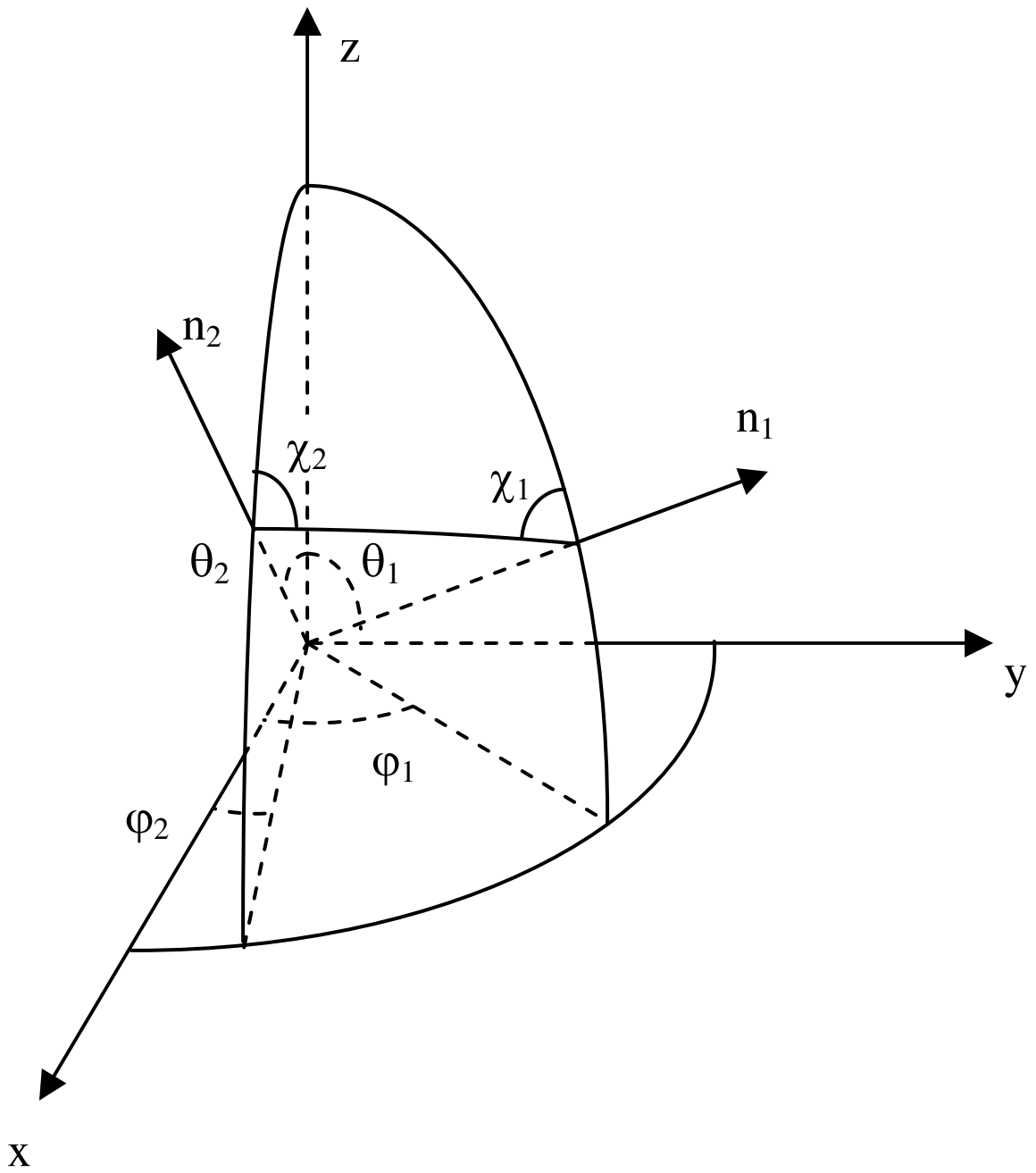


Fig. 1. Geometry of a scattering event. The direction of the incident light is \vec{n}_1 while the scattered light one is \vec{n}_2 ($0 \leq \phi_1 \leq \phi_2 \leq \pi$).

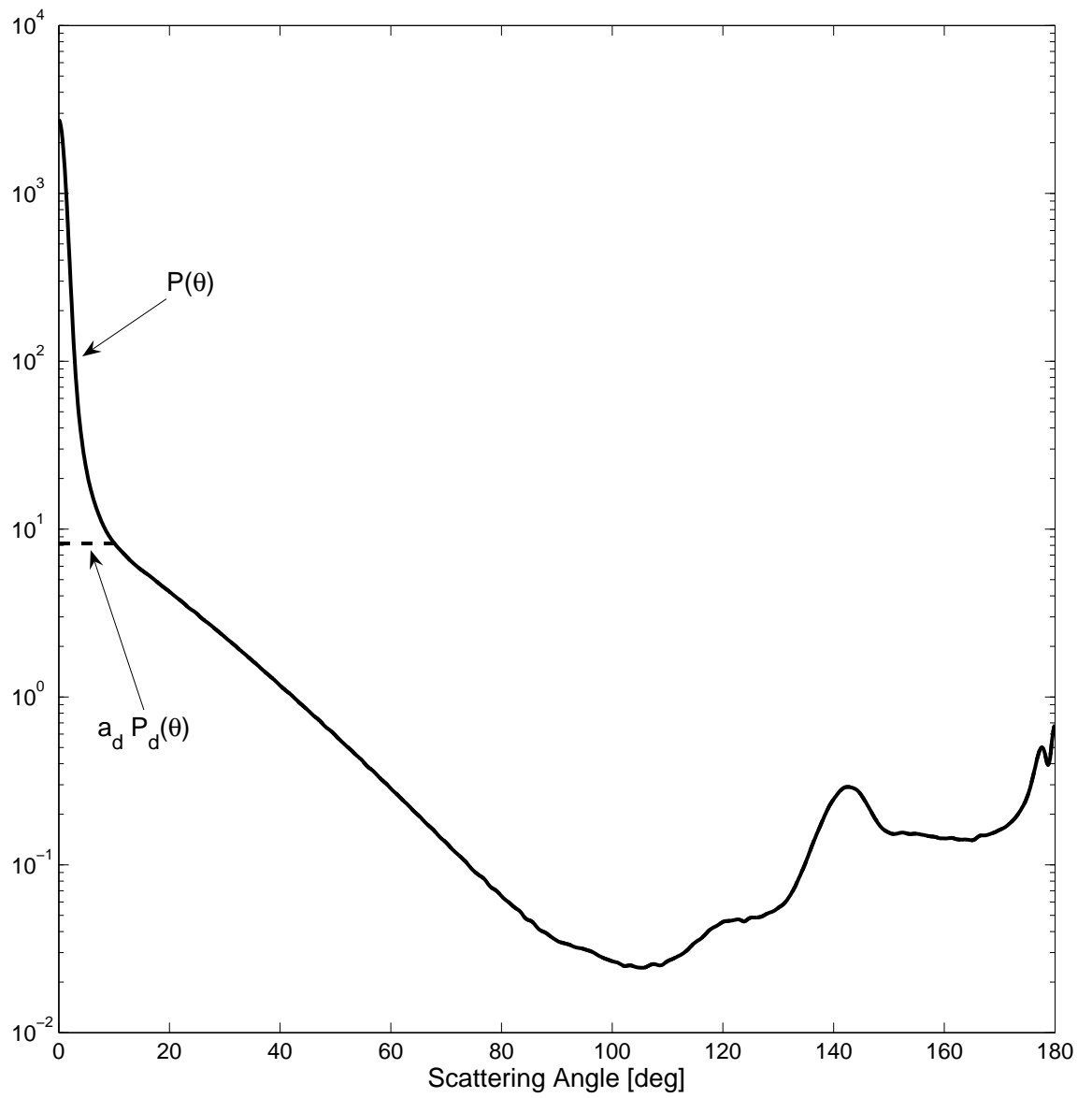


Fig. 2. Phase function of the cloud model Cloud C1 at $0.55 \mu\text{m}$ (solid line) and its diffusion component (dashed line).

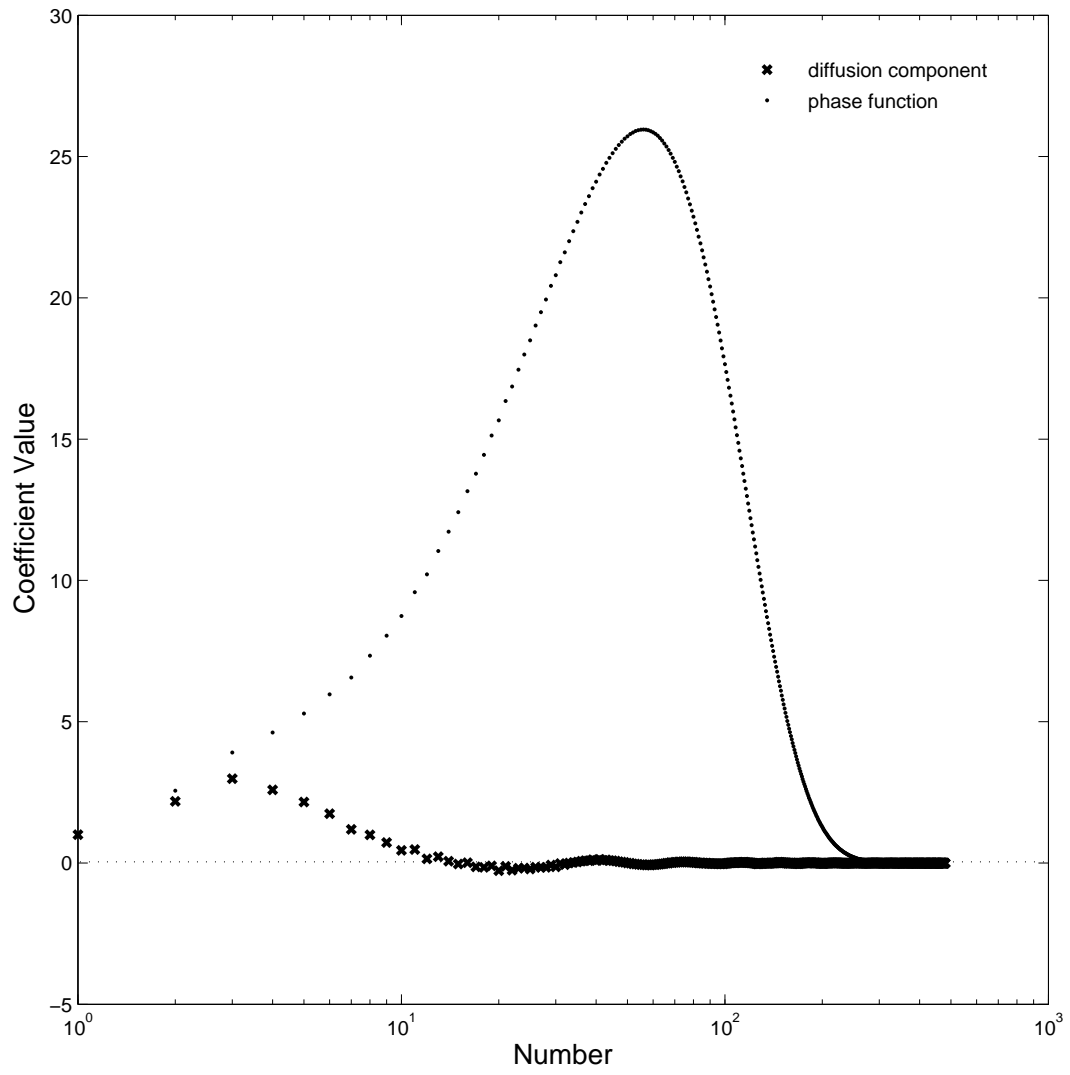


Fig. 3. Coefficients of the decomposition of the phase function (dots) and its diffusion component (crosses) into Legendre polynomials.

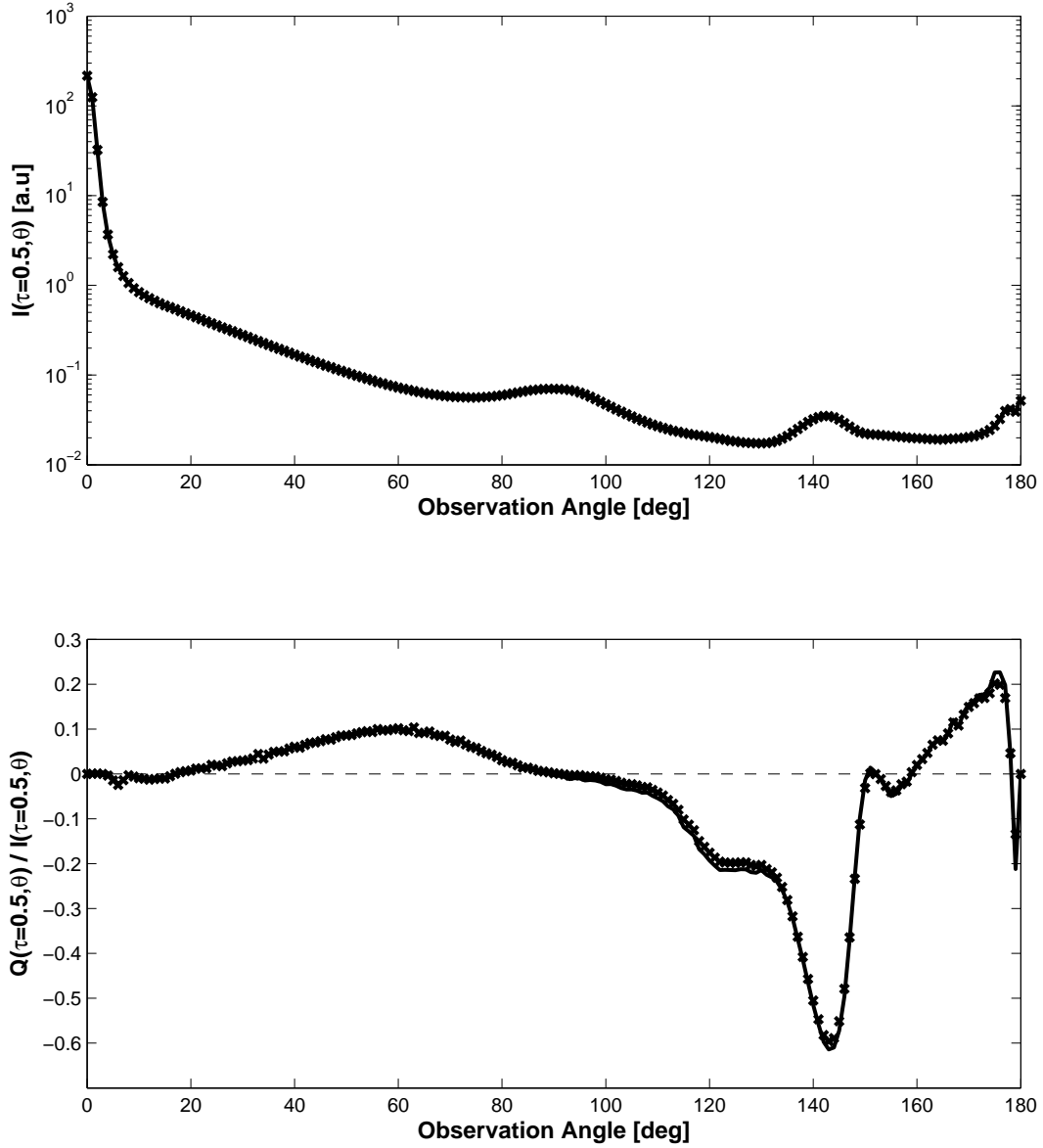


Fig. 4. Component of the Stokes vector I and the ratio Q/I as the function of the observational angle, θ at the level of $\tau = 0.5$. Scattering properties are described by the Deirmendjian cloud model Cloud C.1. at $0.550 \mu\text{m}$. Single scattering albedo is assumed to be 0.95. The total optical thickness of the cloud is 1.0. Sunlight illumination at $\mu_0 = 1.0$. Solid line depicts the accurate simulation results using 200 polynomials and 2 azimuthal harmonics while symbols show results obtained with the use of the small angle approximation and the generalized spherical harmonics calculation using only 20 polynomials and 2 azimuthal harmonics.